Sustainable Food Technology

ROYAL SOCIETY OF CHEMISTRY

PAPER

View Article Online
View Journal | View Issue

Cite this: *Sustainable Food Technol.*, 2025, **3**, 1890

Endophytic fungi-assisted synthesis of chitosan-based cerium oxide nanoparticles for the preservation of postharvest fruits

Bridget Kpomah,†[a] Onome Ejeromedoghene,†*[b] Abiodun Oladipo,[c] Victor Enwemiwe,[d] Muritala Olusola[e] and Sheriff Adewuyi[e]

Received 27th May 2025
Accepted 4th August 2025

DOI: 10.1039/d5fb00240k

rsc.li/susfoodtech

Microbial infestation of postharvest fruits is a serious issue affecting agricultural production and the quality of fresh fruits, especially in areas without advanced storage technologies. This study presents an eco-friendly approach using endophytic fungal (*Aspergillus tubingensis*, AT, and *Rosellinia convexa*, RC) extracts, stabilized with biopolymeric chitosan for the synthesis of cerium oxide nanoparticles (CeONPs) for the preservation of postharvest fruits. The CeONPs were prepared by dissolving chitosan in citric acid, followed by the addition of cerium salts and fungal extracts, which facilitated the reduction of Ce^{3+} to Ce^{0}. The nanoparticles were then purified and dried for further characterization. X-ray photoelectron spectroscopy (XPS) analysis confirmed the presence of Ce^{3+} and Ce^{4+} ions, along with Ce–O bonds, while X-ray diffraction (XRD) revealed highly crystalline CeO_2 nanoparticles with crystallite sizes ranging from 72.4 to 96.7 nm. The materials exhibited hydrophilic properties, as evidenced by water contact angles (WCAs) between 58.95° and 69.31°, ensuring effective adhesion to fruit surfaces for fungal inhibition. Additionally, the chitosan-stabilized CeONPs demonstrated significant antifungal activity, reducing moisture loss and extending the shelf life of cherry tomatoes and grapefruits during storage. This study highlights a sustainable and efficient method for postharvest fruit preservation using biogenic CeONPs.

Sustainability spotlight

This innovative approach leverages endophytic fungi to sustainably synthesize chitosan-based cerium oxide nanoparticles (CeONPs), offering an eco-friendly solution to reduce postharvest fruit losses. Chitosan, a biodegradable polymer, and cerium oxide, known for its antioxidant/antimicrobial properties, combine to form a protective coating that extends the shelf life of postharvest fruits while minimizing chemical preservatives. The fungal-mediated synthesis reduces energy consumption and toxic byproducts compared to traditional methods. By enhancing food security and reducing waste, this technology supports sustainable agriculture and aligns with circular economy principles, contributing to United Nations Sustainable Development Goals, SDGs 2 (Zero Hunger) and 12 (Responsible Consumption). This technique, which uses green materials, is an example of sustainable innovation at the nexus of biotechnology and nanotechnology.

1. Introduction

Most fruits are perishable due to their high water content, which accelerates their deterioration during postharvest storage.[1] This deterioration is frequently brought about by fungal decay that has evolved various strategies for attacking crops by breaking in and snatching nutrients necessary for their growth and development, and the resulting fruit decay typically leads to significant losses in agricultural output and economy.[2] Therefore, to increase the shelf life and nutritional value of vulnerable fruits, it is imperative to design appropriate packaging and storage materials.

Over the years, natural plant extracts and beneficial microorganisms have demonstrated significant potential as fungicides to combat fungal infections in agriculture. However, some plants may develop natural resistance over time by producing defense molecules that protect them against invasive fungal pathogens.[3–5] To address these challenges, phytonanotechnology has emerged as a promising solution for managing and

[a]*Department of Chemistry, Delta State University, PMB 1, Abraka, Nigeria*

[b]*State and Local Joint Engineering Laboratory for Novel Functional Polymeric Materials, College of Chemistry, Chemical Engineering and Materials Science, Soochow University, 215123 Suzhou, Jiangsu Province, P. R. China. E-mail: oejeromedoghene@suda.edu.cn*

[c]*Co-Innovation Center for Sustainable Forestry in Southern China, College of Forestry, Nanjing Forestry University, Nanjing 210037, China*

[d]*Department of Animal and Environmental Biology, Delta State University, PMB 1, Abraka, Nigeria*

[e]*Department of Chemistry, College of Physical Sciences, Federal University of Agriculture, PMB 2240, Abeokuta, Ogun State, Nigeria*

† Equal first author.

detecting crop and fruit diseases both pre- and post-harvest. This innovative approach combines plant extracts with nanoparticles or nanomaterials containing bioactive compounds, which can effectively interact with and target phytopathogen vectors, offering a sustainable and efficient disease management strategy.[6,7]

Even though synthetic agrochemical compounds like pesticides, fungicides, herbicides, and insecticides are widely used for the control and management of phytopathogens in pre- and post-harvest fruits, their careless application has led to unfavorable environmental contamination and further affects non-target microorganisms.[8] Also, many pathogens and pests may have developed resistance and recurrence to these synthetic chemicals.[9] Thus, bio-friendly and biocontrol strategies have emerged as a significant and promising approach for the mitigation of phytopathogens.[10]

By exploring bio-friendly and biocontrol approaches, chitosan, a natural linear polysaccharide (biopolymer), and the second most abundant biopolymer after cellulose, found in the exoskeletons of crustaceans (*e.g.*, shrimp and crab), insect cuticles, and fungal cell walls, has been used extensively to prepare many biochemical compounds for numerous applications. It is non-toxic, biodegradable, and can serve as a biocompatible framework for the synthesis of nanocomposites for phytopathogen management.[11,12]

Notwithstanding, endophytes, especially those isolated from medicinal plants, contain potent secondary metabolites that have been widely utilized in agriculture, biomedicine, and food processing.[13] Numerous studies have been conducted on these metabolites, which contain plant bioactive chemicals like phenols, alkaloids, steroids, flavonoids, and terpenoids, and have shed light on their intricate production pathways.[14] For example, the fungus *Aspergillus tubingensis* produces a variety of bioactive phytochemicals, approximately 20% of which are terpenoids.[15] These compounds—including fonsecin, asperazine, pyranonigrin A, 3,7-diacetamido-7*H*-*s*-triazolo[5,1-*c*]-*s*-triazole, 1,6-dideoxy-L-mannitol, and *cis*-9,10-epoxyoctadecan-1-ol—exhibit antifungal, antibacterial, antipyretic, and even anticancer properties.[16,17] Although there are limited studies on the bioactive compounds of *Rosellinia* spp., phytochemicals including cyclooctadepsipeptide, alkaloid, rosellisteroid, and the cichorine derivative 2, among others, have been derived from extracts of *Rosellinia* spp.[18]

Many recent studies have examined new methods for targeted synthesis of these vital metabolites using a variety of biotechnological instruments, which allow for the regulated synthesis of agrochemical materials with greater efficacy,[19] especially by exploring these bioactive compounds as eco-friendly materials for developing novel nanoparticles.[20,21]

The combination of chitosan and inorganic nanoparticles is important in current research because they exhibit strong antimicrobial properties that can effectively inhibit the growth of bacteria, fungi, and other pathogens responsible for post-harvest spoilage. The bioactive content can be released in a controlled manner, ensuring long-lasting protection during storage and transportation. These materials also possess antioxidant properties that scavenge reactive oxygen species (ROS), reducing oxidative damage to fruits and vegetables and maintaining their freshness.

Previous studies have established chitosan-stabilized bismuth and zirconium nanoparticles as potent antifungal agents against *B. cinerea* for the preservation of postharvest cherry fruits with shelf life preservation of up to 10 d under normal environmental conditions.[22] Moreover, the dragon fruit stem extract has been examined as a reducing agent for the synthesis of silver nanoparticles and incorporated into a chitosan-based film as a potential packaging material for extending the shelf life of postharvest strawberry fruits during storage.[23] Furthermore, modified chitosan-stabilized zinc oxide nanoparticles assisted by hydrogen were reported to significantly enhance the quality and nutritional content of tomato fruit during storage.[24] Similarly, the fabrication of chitosan oligosaccharide–zinc oxide nanocomposites was seen to improve the quality of tomato fruits during postharvest storage.[25] Chitosan–iron oxide nanoparticles have demonstrated effectiveness in controlling soft rot disease in peach fruits, with their efficacy dependent on concentration and application timing. Studies indicate that 1% chitosan–iron oxide nanoparticle treatment inhibits fungal growth and suppresses fruit respiration by forming a protective chitosan surface layer, thereby significantly reducing weight loss during storage.[26]

Nevertheless, studies involving chitosan–cerium acetate coatings have demonstrated fruit firmness, reduced weight loss, enhanced antioxidant enzyme activity, and preserved nutrients (vitamin C and lycopene) in cherry tomatoes;[27] meanwhile, water-soluble chitosan–cerium complexes could improve the shelf life of cherry tomatoes and degrading pesticide residues, showing cerium's strong preservation capabilities.[28,29] To the best of our knowledge, no studies have directly addressed the combination of endophytic fungi-assisted synthesis of cerium oxide nanoparticles (CeONPs) integrated into chitosan matrices for spraying post-harvest preservation of cherry tomatoes (*Solanum lycopersicum* var. *cerasiforme*) or grapefruits (*Vitis vinifera*). However, related work supports the potential of chitosan–CeO_2 coatings for microbial spoilage reduction and shelf life extension.[30]

2. Materials and methods

2.1 Materials

Analytical grade reagents were used as received for the experiment without further purification. The chemicals include chitosan (100–200 mPa s, 95%) purchased from Shanghai Aladdin Biochemical Technology Co., Ltd, China, citric acid anhydrous (99.5%) obtained from Shanghai Lingfeng Chemical Reagent Co. Ltd (Shanghai, China), and ammonium cerium nitrate procured from TCI Chemicals, Shanghai, China. Ethanol (99.7%) of analytical purity was procured from Sinopharm Chemical Reagent Co. Ltd Shanghai, China. Double-distilled water was used for the preparation of all aqueous solutions.

2.2 Preparation of fungal cultures and extracts

Fresh leaves of *Gingko biloba* were obtained from Nanjing Forestry University, China. The leaves were sterilized with 70%

alcohol and 2% sodium hypochlorite for 60 s and 180 s, respectively. Thereafter, the sterile leaves were rinsed thrice in sterilized distilled water to separate the extra surfactant and dried in an ultra-clean environment. Next, the leaves were cut into 1 cm^2 using a sterilized scalpel, transferred to a plate containing potato dextrose agar (PDA), and cultured in an incubator at 28 °C for 3 days without light. The pure fungal colonies were cultured in PDA plates and further identified as *Aspergillus tubingensis* and *Rosellinia convexa*; organic crude extracts of the mycelium of both fungi were extracted following previously reported methods with slight modification,[31] and the extracts were stored for further use.

2.3 Preparation of chitosan–cerium oxide nanoparticles

First, a homogeneous chitosan (Chit) solution was prepared by dissolving 1.0 g of Chit in 0.1 M citric acid solution (100 mL) in a round-bottom flask placed in a temperature-controlled oil bath at 70 °C for 2 h under magnetic stirring. To 25 mL of the Chit solution, 1.0 mM cerium salts were introduced with continuous stirring for 1 h. Next, 10 mL of the freshly prepared fungal (*Aspergillus tubingensis*, AT, and *Rosellinia convexa*, RC) extract solution was added carefully, and the reaction was allowed to proceed for another 1 h to allow the reduction of Ce^{3+} to Ce^0.[32] The CeONPs were collected by centrifuging the obtained mixture, while the supernatant was decanted. The CeNPs obtained were washed with ethanol to remove impurities and vacuum-dried at 60 °C for 6 h. The obtained nanoparticles were designated as Chit–CeONPs, Chit–AT CeONPs, and Chit–RC CeONPs (Table 1 and Scheme 1).

2.4 Characterization of the prepared nanoparticles

The samples were characterized by measuring the absorbance using a UV-2600 Shimadzu, Japan, in the wavelength range of 200–800 nm. The presence of functional groups was determined on a TENSOR27 PMA 50 Fourier transform infrared (FT-IR) spectrophotometer (Brook, Germany) at a resolution of 4.0 cm^{-1} over 32 scans from 4000 to 400 cm^{-1}. The electronic state of the elemental species was studied with a Thermo Scientific ESCALAB 250 XI X-ray photoelectron spectrometer. Thermogravimetric analysis (TGA) and derivative thermogravimetric (DTG) analysis were performed at a heating rate of 10 °C min^{-1} and from 30 to 500 °C, under a nitrogen atmosphere on a NETZSCH TG 209F3 instrument. The morphology features were analyzed on a Nova NanoSEM 450 scanning electron microscope coupled with an energy-dispersive X-ray (EDX) spectrometer. The crystalline features were assessed using a Bruker-AXS X-ray diffractometer at a scan speed of 10° min^{-1} from 5° to 80°. The water contact angle (WCA) was studied on a SL200C, KINO Industries Inc., USA.

2.5 Postharvest fruit preservation studies

Fresh postharvest cherry tomatoes and grapefruits were purchased from the Soochow University fruit shop. The fruits were properly washed with distilled water and allowed to dry at room temperature. Thereafter, the fruits were distributed into five groups (containing 5 fruits per group) and sprayed with 10 mL of the as-prepared CeONP solution on the first day, stored under ambient environmental conditions (70% relative humidity and 25 °C room temperature), and observed daily for up to 35 days. The first group, which served as the control group, was unsprayed. The other groups were sprayed with pure chitosan solution, Chit–CeONPs, Chit–AT CeONPs, and Chit–RC CeONPs, respectively. After several days of observation, the percentage of fruit spoilage evidence and severity was determined by weight loss due to a reduction in moisture content according to eqn (1):

$$S = \left[\left(\frac{W_o - W_m}{W_o}\right) \times 100\right] \quad (1)$$

where S is the severity of fruit spoilage, W_o is the original weight of the fresh fruit, and W_m is the average weight loss in moisture content during storage.[33] The test was done in triplicate, and results were presented as mean ± standard error.

3. Results and discussion

3.1 UV optical characteristics

The UV-vis characterization of the CeONPs displayed characteristic absorbance peaks at wavelengths below 400 nm as expected.[34] According to UV-vis spectra, Chit–CeONPs displayed a maximum absorption at 230 nm; however, Chit–AT CeONPs and Chit–RC CeONPs displayed broad maximum absorption at 275 and 272 nm, respectively (Fig. 1a). The observed absorption maxima are associated with the intrinsic absorption band-gap of CeONP powder that is facilitated by the electronic transition occurring within the valence and conduction bands. Moreover, the absorption observed at 301 nm in Chit–AT CeONPs could be due to the charge transfer from O 2p to Ce 4f in cerium oxide.[35]

Furthermore, the optical band gap energy (E) of the synthesized CeONPs was calculated from the wavelength (λ) obtained from the UV-vis data according to eqn (2);

$$E = \frac{1240}{\lambda} \quad (2)$$

Table 1 Composition of various samples

Sample	Chitosan (g)	Citric acid (M)	Cerium salt (mM)	Fungal extracts (10 mL)
Chit–CeONPs	1.0	0.1	1.0	—
Chit–AT CeONPs	1.0	0.1	1.0	*Aspergillus tubingensis*
Chit–RC CeONPs	1.0	0.1	1.0	*Rosellinia convexa*

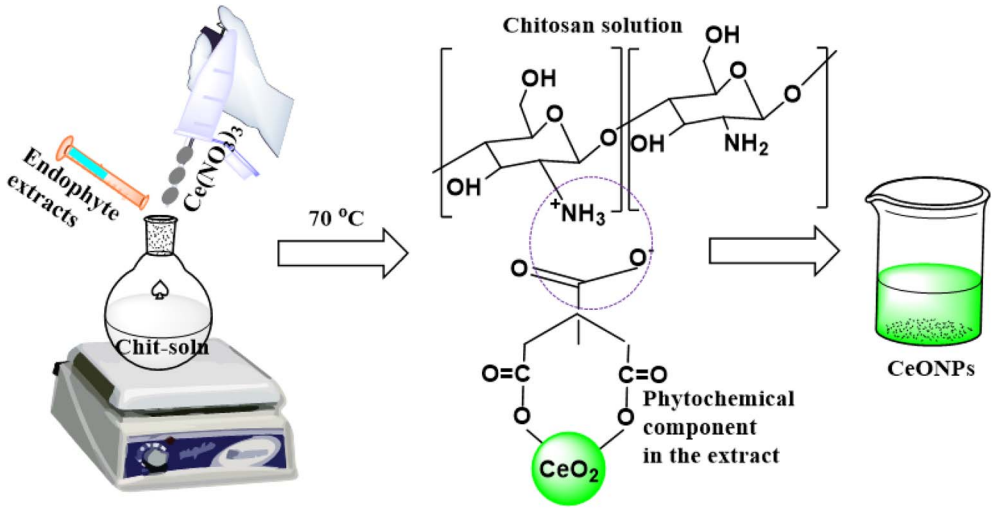

Scheme 1 The preparation process of chitosan-based cerium oxide nanoparticles aided by bioactive extracts.

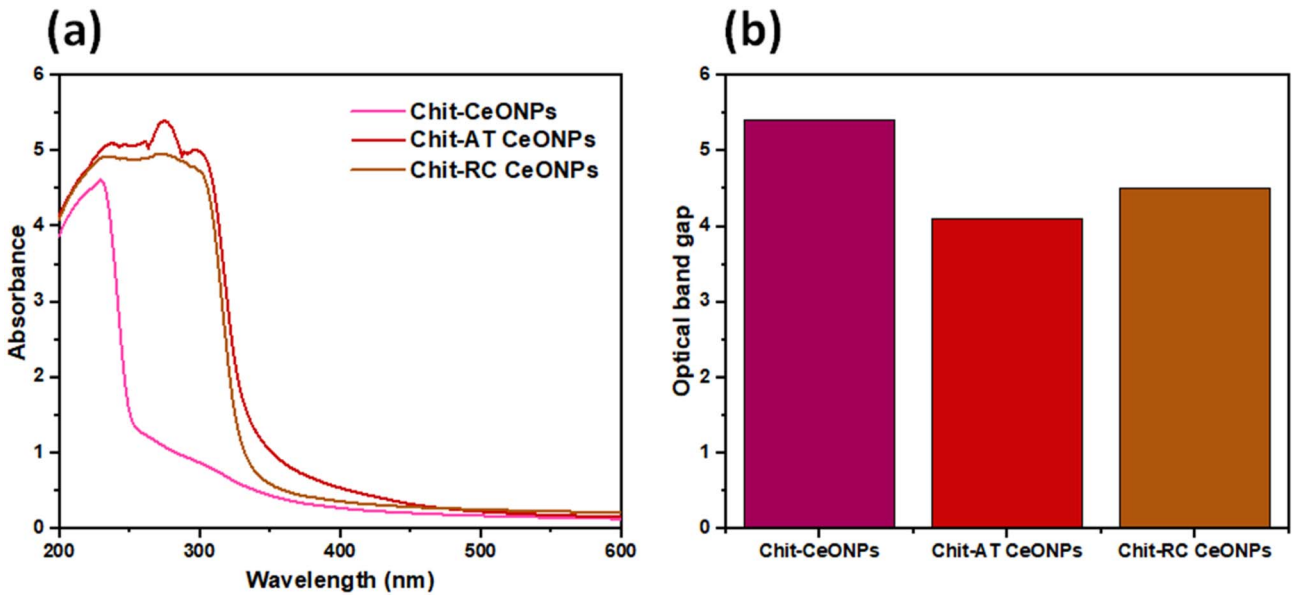

Fig. 1 UV-vis spectroscopic study showing (a) electronic absorption and (b) optical band gap of the synthesized CeONPs.

The obtained optical band gap was 5.4, 4.1, and 4.5 eV for Chit–CeONPs, Chit–AT CeONPs, and Chit–RC CeONPs, respectively (Fig. 1b), which are larger than the value (3.2 eV) obtained for bulk CeO_2. The increase in the optical band gap for the CeONPs could be ascribed to the surface defects due to oxygen vacancies in the Ce^{3+} state. Typically, the Ce^{3+}/Ce^{4+} ratio increases near the surface, creating localized defect states within the band gap. Moreover, the presence of hydroxyl (–OH) or carbonate ($-CO_3$) groups on nanoparticle surfaces can introduce new electronic transitions, shifting the absorption edge.[36]

3.2 Structural characteristics

The chemical structure characterization of the materials based on FTIR studies shows the presence of interacting functional groups in the materials.[37] Typically, strong overlapping –OH and –NH vibrational modes were observed around 3452–3445 cm^{-1} in the materials. The sharp and strong amide (C=O) bond was obtained at 1632–1623 cm^{-1} and the –NH deformation band at 1460–1456 cm^{-1} in the materials. Furthermore, the weak vibrational frequency due to –NH deformation occurring at 1379 cm^{-1} in Chit–CeONPs was significantly intensified and shifted to 1388 cm^{-1} in Chit–AT CeONPs and Chit–RC CeONPs, showing good interaction of the endophytic fungi in the reaction process (Fig. 2). The bands that occurred at 1239–1227 cm^{-1} and 1127–1125 cm^{-1} could be due to the interaction of C–O–C and C–N bonds, while the stretching of Ce–O bonds was observed at 593–515 cm^{-1}.[38]

Furthermore, XPS studies were performed to ascertain the interfacial elemental composition and interaction of the

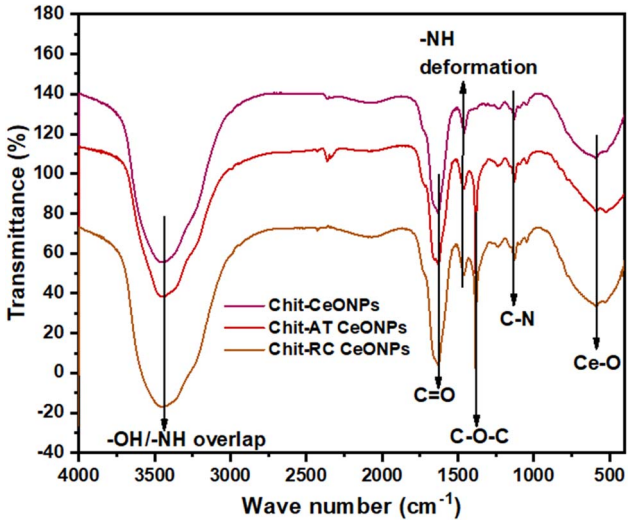

Fig. 2 FTIR spectra of the synthesized CeONPs.

materials. The XPS low-resolution full survey scan spectra show the presence of major interacting components (C 1s, N 1s, O 1s, and Ce 3d) in the materials with slight differences in the peak intensities (Fig. 3a–c). The deconvolution of the high-resolution XPS spectrum of cerium in Chit–CeONPs shows the Ce 3d spin–orbit components with the binding energies of ~883 and ~885 eV, which are typical for Ce $3d_{5/2}$ splitting for cerium oxide compounds; however, Ce 3d spin–orbit components for Chit–AT CeONPs and Chit–RC CeONPs were observed at binding energies of ~884 and ~902 eV, respectively (Fig. 4a(i)–(iii)). The well separated spin–orbit components correspond to the Ce $3d_{5/2}$ and Ce $3d_{3/2}$ splitting, respectively, due to Ce^{3+} and Ce^{4+} ions in CeO_2 compounds.[39] These peaks were characterized by intense absorption and corresponded to the splitting of CeO_2. The XPS survey scan for O 1s of the materials shows a strong peak at ~530 eV, which is due to a metal–oxygen (Ce–O) bond, showing the formation of metal oxide nanoparticles (Fig. 4b(i)–(iii)). Moreover, in the N 1s spectra of Chit–CeONPs, the single intense peak at ~398 eV binding energy could be due to the organic C–NH_2 group of chitosan in the material. Similarly, Chit–AT CeONPs and Chit–RC CeONPs demonstrated an intense peak at ~398 eV binding energy as well as a new peak at ~406 eV binding energy (Fig. 4c(i)–(iii)). The occurrence of the new peak could be due to the presence of nitrogen-containing aromatic π–π* satellite features.[40]

In addition, the C 1s spectra of Chit–CeONPs were characterized by a strong peak at ~284 eV due to –C/C–H bonding interactions and a weak peak at ~288 eV, which is assigned to C═O bonds in chitosan.[41] However, the C–C/C–H bonds in Chit–AT CeONPs and Chit–RC CeONPs were shifted to the binding energy of ~283 eV as well as the C═O bonds occurring at ~288 eV; also, a shoulder peak appeared at the binding energy of ~285 eV, which could be associated with C–O–C bonds impacted by the phytochemicals of the plant extracts, as this peak was not obvious in Chit–CeONPs (Fig. 4d(i)–(iii)).

3.3 Thermal characteristics

The thermolysis properties of the materials that reveal the degradation rate at high temperatures were conducted, and the results are presented in the TGA and DTG profiles (Fig. 5a and b). The results show that the materials displayed two stages of degradation. In the first stage, there was a steady loss of physically absorbed water in the material with 83% weight loss at 73 °C. This could be due to the hydrophilic nature of chitosan with numerous hydroxyl (–OH) and amino (–NH_2) groups in its structure. These polar functional groups and the polysaccharide backbone of chitosan have a high affinity for water, contributing to hydration. However, in the second stage of degradation, the weight loss around 73 to 220 °C could be associated with the degradation of the bioactive organic groups attached to the surface of the endophytic fungal extracts/chitosan that are involved in the stabilization and formation of CeONPs.[42]

3.4 Microstructure characteristics

The micromorphological features of the materials were analyzed by scanning electron microscopy (SEM) to provide information on the surface morphology. The surface features of Chit–CeONPs demonstrate a rough surface with stripes and microspheres of uniform distribution, which could be due to the distribution of cerium oxide in the organic–inorganic polymer matrix (Fig. 6a).[22] Moreover, the surface characteristics

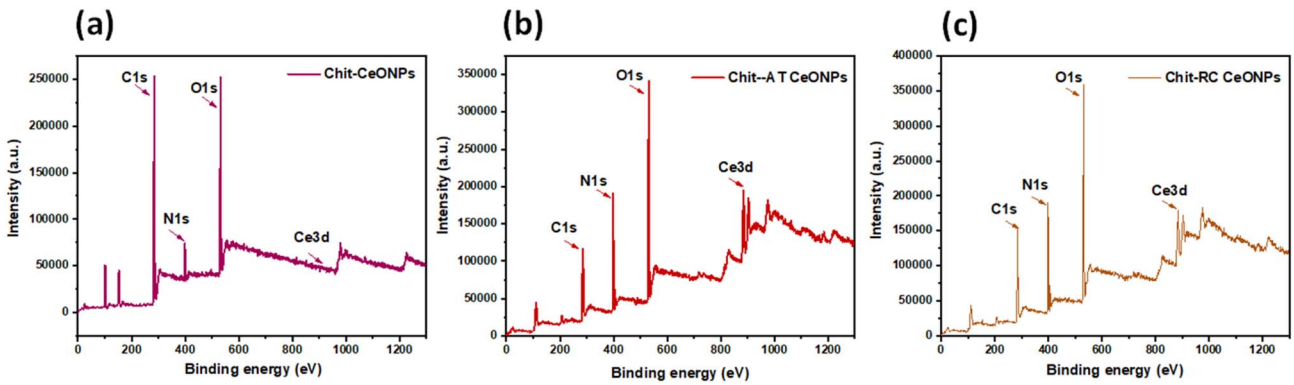

Fig. 3 Low-resolution XPS spectra of (a) Chit–CeONPs, (b) Chit–AT CeONPs and (c) Chit–RC CeONPs.

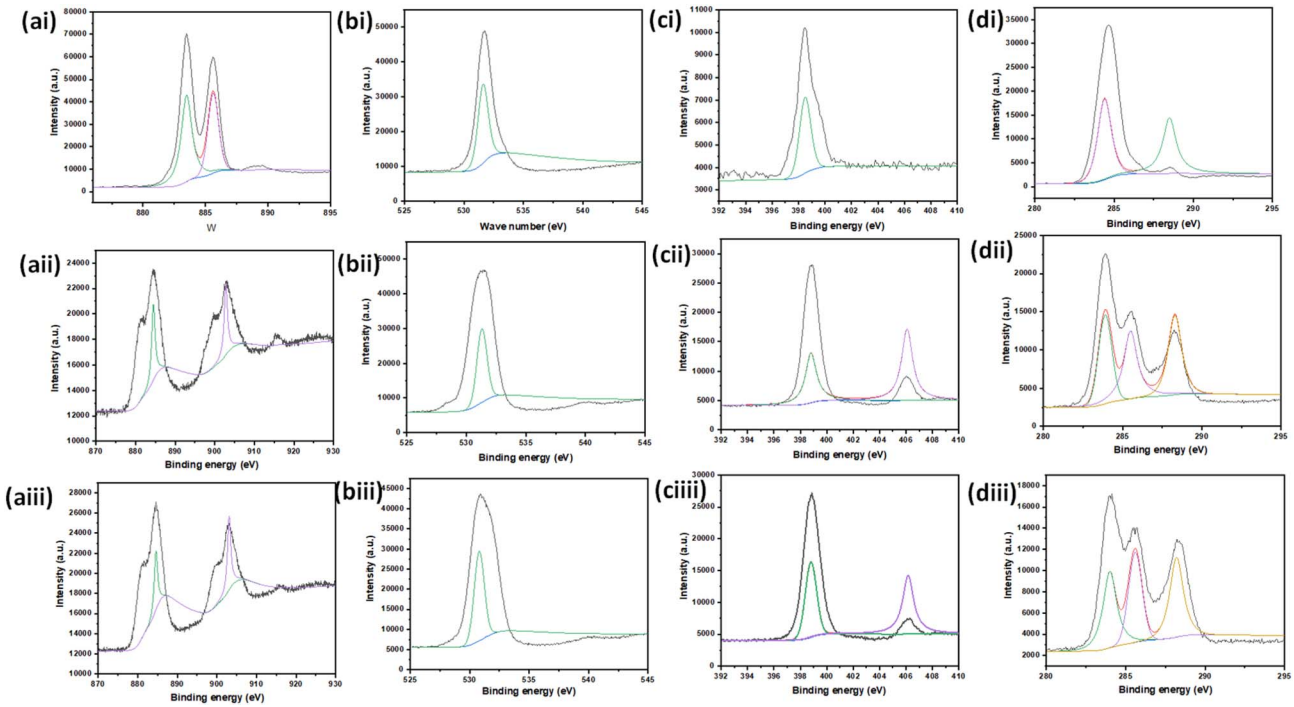

Fig. 4 High-resolution XPS spectra of (i) Chit–CeONPs, (ii) Chit–AT CeONPs, and (iii) Chit–RC CeONPs showing (a) Ce 3d, (b) O 1s, (c) N 1s, and (d) C 1s splitting.

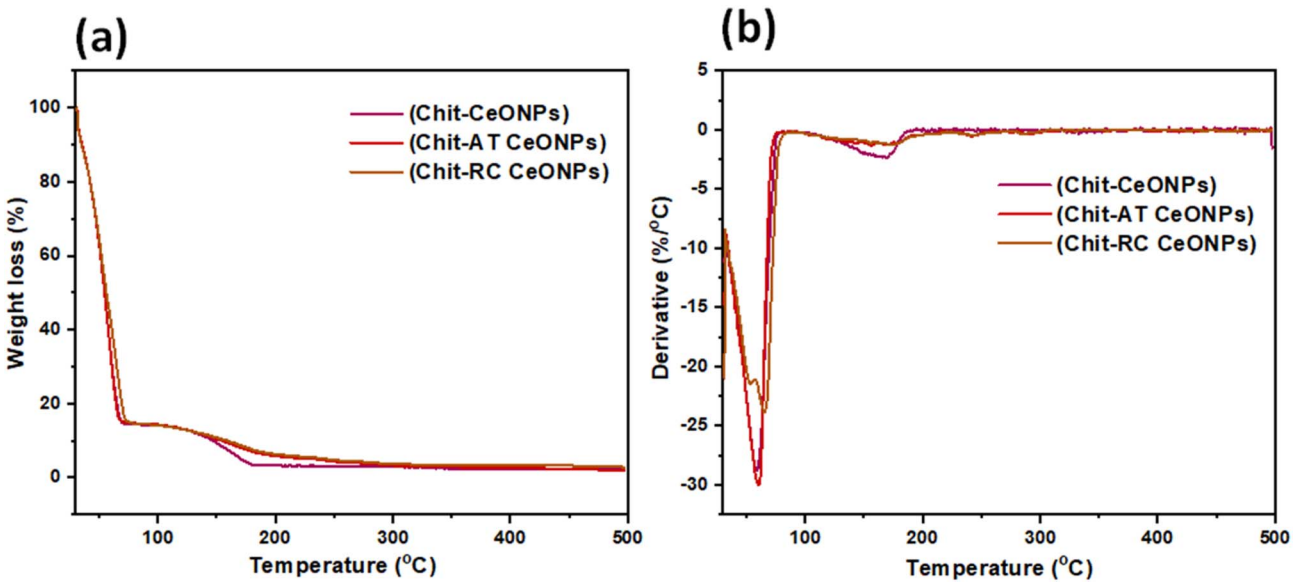

Fig. 5 Thermogravimetric analysis showing the (a) TGA profile and (b) DTG curve of the synthesized CeONPs.

of Chit–AT CeONPs and Chit–RC CeONPs demonstrated morphological changes due to the presence of the plant extract, giving rise to coarse surfaces with a uniform distribution of well-ordered stripes (Fig. 6b and c).

The elemental maps of the materials showed that the primary elemental compositions were uniformly distributed, and CeONPs were well stabilized in the organic–inorganic polymer matrix (Fig. 6d–f). Furthermore, the energy dispersive X-ray (EDX) spectra showed remarkable C, N, O, and Ce composition in all the materials (Fig. 7a–c).[43] Typically, for all the materials, the representative relative weight abundance and atomic percentage were 29–38% for C, 28–31% for N, and 29–32% for O.[44] However, the relative weight abundance and atomic percentage for Ce were ~9% and ~1%, respectively (Fig. 7d and e).

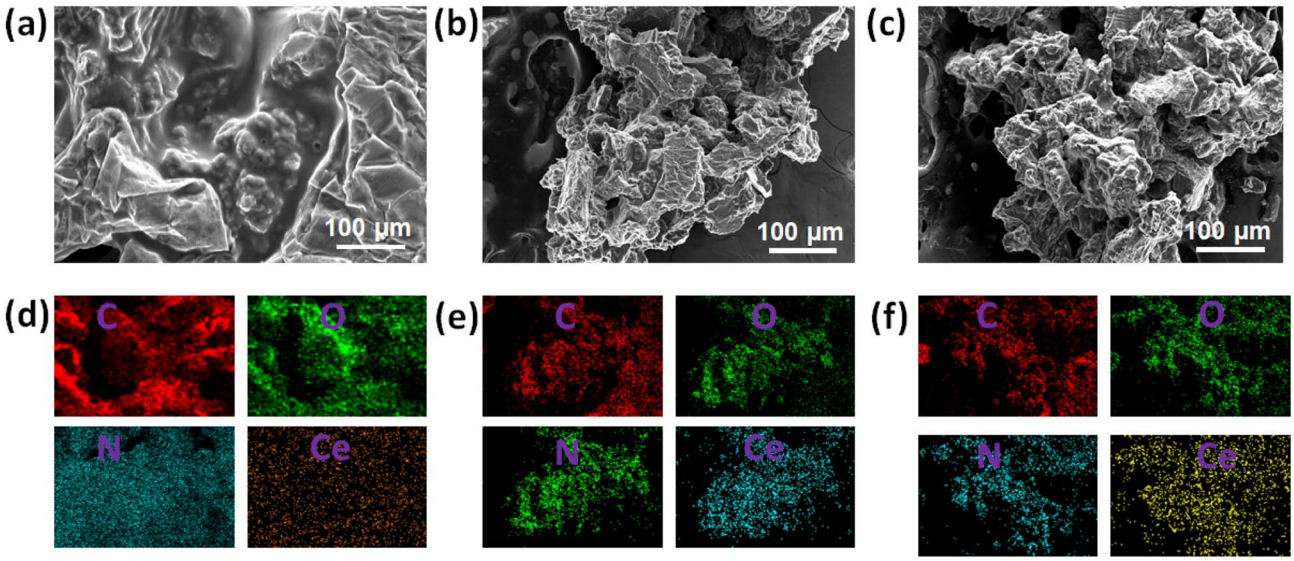

Fig. 6 SEM micrographs/elemental mapping images of (a and d) Chit–CeONPs, (b and e) Chit–AT CeONPs and (c and f) Chit–RC CeONPs.

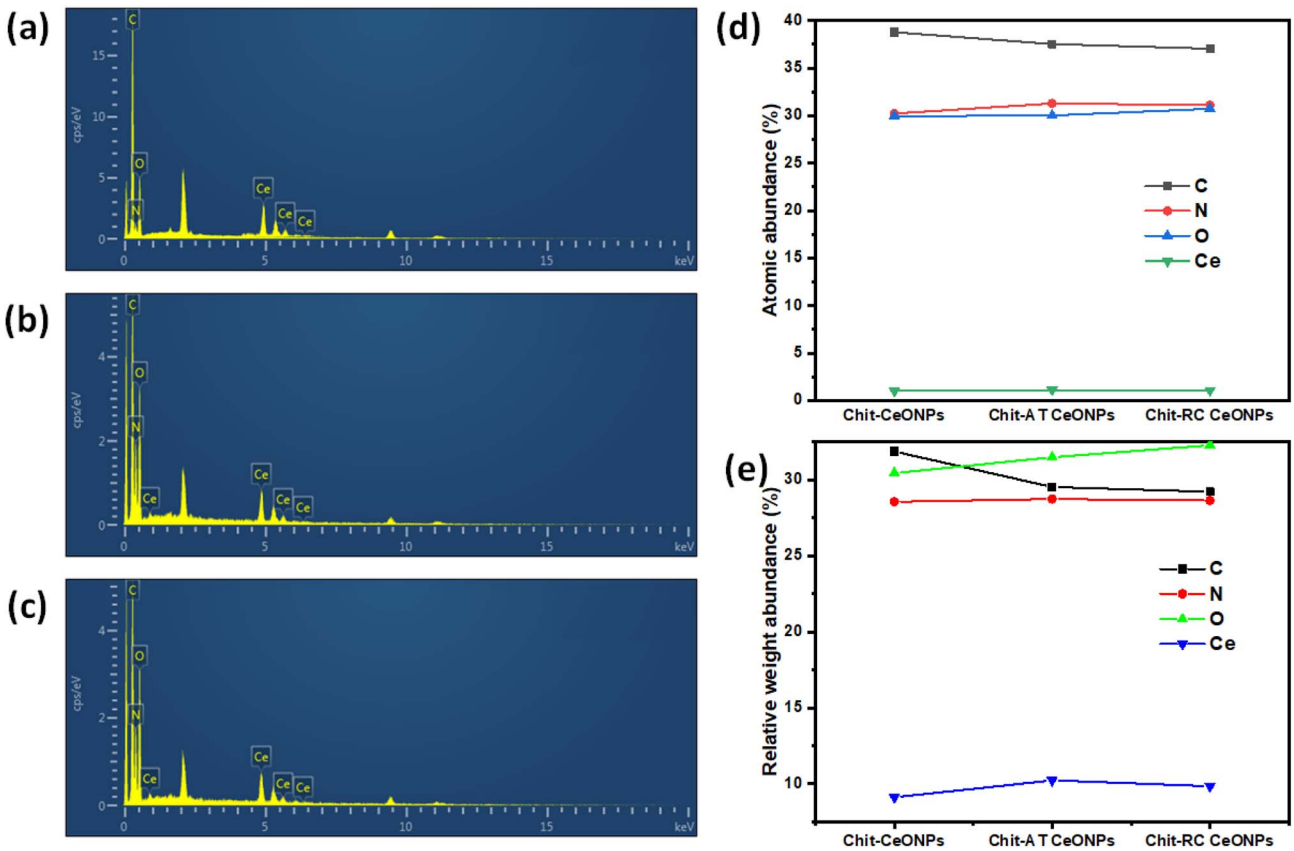

Fig. 7 EDX spectra of (a) Chit–CeONPs, (b) Chit–AT CeONPs and (c) Chit–RC CeONPs. (d) Relative weight abundance and (e) atomic percentage of the materials.

X-ray diffraction (XRD) studies were performed to characterize the crystallinity of the CeONP-based materials (Fig. 8). The materials displayed crystalline diffraction peaks, which differ in intensity. This shows that CeONPs did not contain any contaminants from other species. The XRD profile of Chit–CeONPs displayed a characteristic strong peak at $2\theta = 12.2°$ (100) and a weak peak at $2\theta = 25.8°$. These peaks were shifted to $2\theta = 21.13°$ (110) and $2\theta = 36.7°$ (104), respectively, in Chit–AT

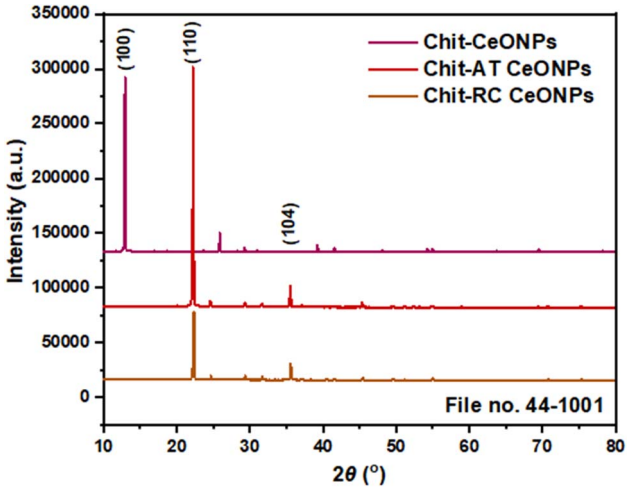

Fig. 8 XRD spectra of the synthesized CeONPs.

CeONPs and Chit–RC CeONPs due to the presence of plant extracts (Monica & Aishah, 2023).[45] The observed diffraction pattern corresponds to the formation of CeO_2 with JCPDS (Joint Committee on Powder Diffraction Standards) file no. 44-1001.

In addition, the average crystallite sizes of the CeONPs, calculated by using the Debye–Scherrer equation, eqn (3), were found to be 72.4, 91.9, and 96.7 nm.

$$D = \frac{k\lambda}{\beta \cos \theta} \quad (3)$$

where D is the average crystallite size (nm), λ is the wavelength of X-ray source (0.15406 nm), k is the Scherrer constant (0.94), β is the full width at half-maximum (FWHM) data with intensity and position provided by XRD patterns (radians), and θ is the Bragg diffraction angle/peak position (radians). The obtained average crystallite sizes show evidence of the association of the bioactive extract with ceria, validating their interaction in the synthesis of CeONPs.[46]

3.5 Hydrophilicity/wetting properties of the nanoparticles

To determine the stability of the CeONPs and their adhesive properties on the surface of post-harvested fruits when applied by spraying, the water contact angle (WCA) of the materials was measured.[47] Studies have shown that as the WCA decreases from 90°, its hydrophilic nature increases.[48] Therefore, we observed that Chit–CeONPs were less hydrophilic with a recorded contact angle of 69.31° (Fig. 9a); meanwhile, Chit–AT CeONPs and Chit–RC CeONPs showed WCAs of 58.95° and 64.95°, respectively (Fig. 9b and c). The results show increased stability of the nanoparticles as well as good wetting and hydrophilic properties of the materials, showing that the nanoparticle solution can spread completely on the fruits' surfaces to inhibit the growth of fungi during storage.[49]

3.6 Fruit preservation studies

During postharvest storage, the most observable variable for assessing fruit spoilage is weight loss, which is often due to loss of water and the respiratory cycles that convert glucose to CO_2 (Fig. 10a).[50] This causes the fruits to become soft and unappealing. The process of spoilage during storage results from a series of physicochemical reactions and rotting microorganisms affecting the tissues of fruits.[51] The growth and development of these microorganisms change due to changing environmental conditions of temperature and humidity, affecting the stored fruits' pH and color.[52]

In the process of storage, for the cherry tomato fruits, the loss of moisture was experienced in the control group after seven days of storage. This group experienced gradual weight loss, with dark patches on the surface due to microbial infestation; meanwhile, the other groups remained fresh (Fig. 11a). The loss in moisture in the tomatoes could be ascribed to the enzymatic degradation of pectin present in the cell wall *via* enzymes like pectin methyl esterase and polygalacturonase.[53]

Moreover, the grape control group displayed gradual discoloration after 3 days, followed by the gradual growth of mold as fuzzy gray patches on the surface of fruits. This was also accompanied by a mushy and wrinkled texture or leaky juice (Fig. 11b). The degradation of the grapefruit could be due to an increase in oxygen consumption due to the low rate of aerobic respiration of grapefruit as the spoilage progresses. The spoilage and the increase in the number of aerobic microorganisms increased the oxygen consumption, leading to spoilage.[54]

The determination of the extent of disease evidence and severity was achieved by weight loss, resulting in a decrease in

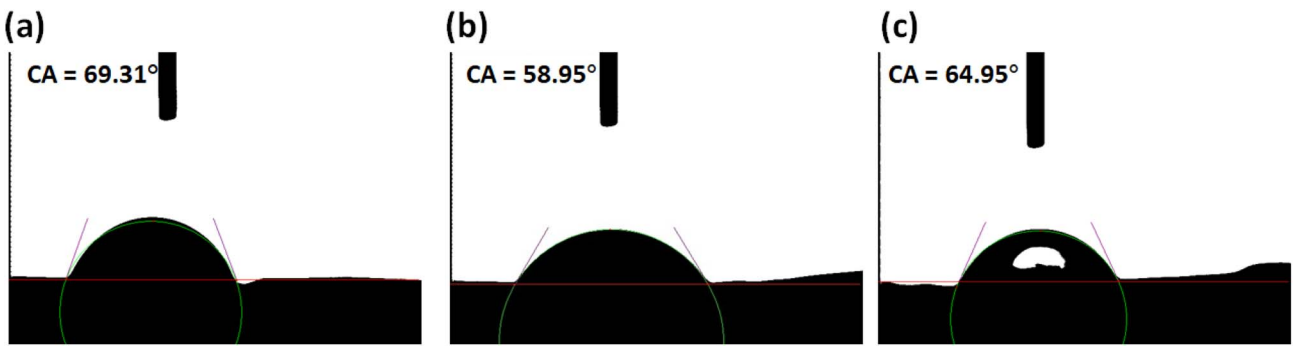

Fig. 9 Water contact angle (CA) of (a) Chit–CeONPs, (b) Chit–AT CeONPs and (c) Chit–RC CeONPs.

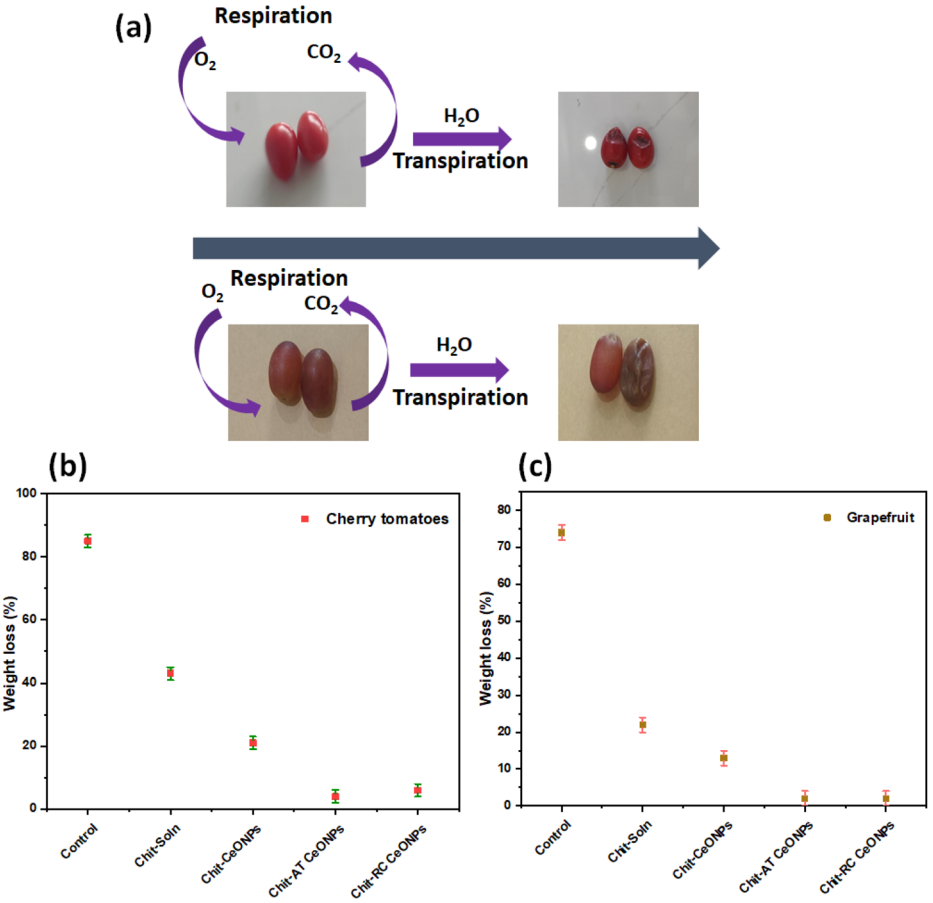

Fig. 10 Images showing (a) the process of fruit degradation due to a high rate of respiration. Percentage of disease evidence and severity due to loss in moisture/weight loss in (b) cherry tomatoes and (c) grapefruits.

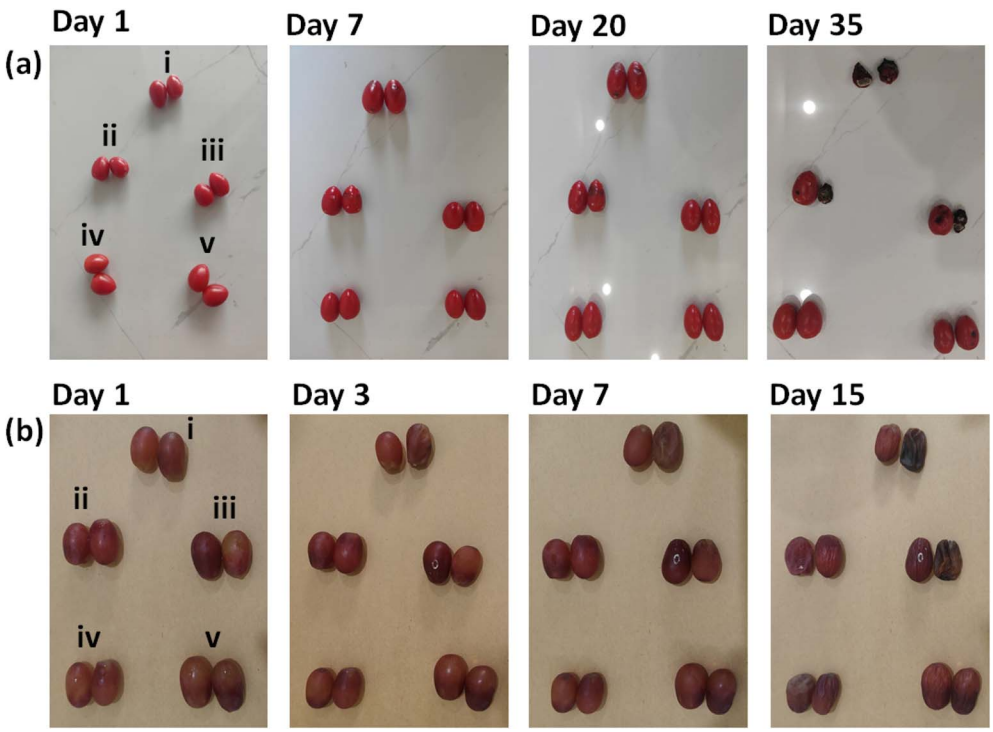

Fig. 11 Postharvest fruit preservation of (a) cherry tomatoes and (b) grapefruits: (i) control group (unsprayed), (ii) sprayed with pure chitosan solution, (iii) sprayed with Chit–CeONPs, (iv) sprayed with Chit–AT CeONPs, and (v) sprayed with Chit–RC CeONPs.

moisture content during postharvest storage. The results show that the control group recorded 85% weight loss in cherry tomato fruits after 35 days. Nevertheless, the fruits that were preserved with pure chitosan, Chit–CeONOs, Chit–AT CeONPs, and Chit–RC CeONPs demonstrated 43%, 21%, 4%, and 6% decrease in moisture content by weight loss, respectively, on the same day (Fig. 10b). Moreover, the control group in the grapefruits recorded 74% weight loss after 15 days; while the ones preserved with pure chitosan, Chit–CeONOs, Chit–AT CeONPs, and Chit–RC CeONPs demonstrated 22%, 13%, 2%, and 2% loss in moisture content, respectively, on the same day (Fig. 10c).

To verify whether the CeONPs were absorbed or remained on the fruit surface, a simple rinse-and-observe test was carried out. Herein, after spraying the CeONP solution on the fruit surface, it was allowed to dry for at least 10 days. Thereafter, the fruits were gently rinsed with distilled water and mild buffer pH 7. After observation, the water/buffer solution became cloudy with visible tiny residues. This suggests that the nanoparticles loosely adhered to the surface of the fruit and not adsorbed.[55]

4. Conclusion

The study demonstrates that the application of endophytic fungi-assisted synthesis of chitosan-based cerium oxide nanoparticles (CeONPs) for the preservation of postharvest fruits could help tackle or delay post-harvest fruit rot, mainly caused by moisture loss and pathogenic microbes. Herein, freshly prepared fungal (*Aspergillus tubingensis*, AT, and *Rosellinia convexa*, RC) extract and chitosan solution were explored for the preparation of CeONPs with optical band gap properties (4.1–5.4 eV) larger than that of bulk CeO_2 (3.2 eV). This value reflects the quantum size effect or the charge transition of ions observed in Ce^{3+} and Ce^{4+}. The micromorphological features of the materials reveal coarse surfaces with a uniform distribution of well-ordered stripes, which could be attributed to the presence of plant extracts. Furthermore, the XRD spectra show sharp crystalline diffraction peaks attributed to pure CeONPs free from contaminants that may arise from other species in the material. In addition, the water contact angle studies reveal the formation of stable nanoparticles as well as good wetting and hydrophilic properties that can spread uniformly and completely when applied on fruit surfaces to help inhibit the growth of fungi during storage. This study revealed that endophytic fungi-assisted synthesis of chitosan-based CeONPs could significantly enhance perishable fruits' firmness with minimal moisture loss, thus improving the shelf life of the fruits during storage. In addition, it will be interesting to optimize fungal strains and synthesis conditions to scale up eco-friendly production.

Conflicts of interest

The authors declare that they have no known competing financial interests or personal relationships that could have appeared to influence the work reported in this paper.

Data availability

Data will be made available on request.

Acknowledgements

This work was financially supported by the Jiangsu Outstanding Postdoc Program with grant number 2024ZB885.

References

1 R. Lufu, A. Ambaw and U. L. Opara, *Sci. Hortic.*, 2020, **272**, 109519.
2 J. G. de Oliveira Filho, G. da C. Silva, L. Cipriano, M. Gomes and M. B. Egea, *J. Food Sci.*, 2021, **86**, 3341–3348.
3 S. Kaur, M. K. Samota, M. Choudhary, M. Choudhary, A. K. Pandey, A. Sharma and J. Thakur, *Physiol. Mol. Biol. Plants*, 2022, **28**, 485–504.
4 X. Qi, B. Chen and J. Rao, *Curr. Opin. Food Sci.*, 2023, **52**, 101054.
5 N. A. Matrose, K. Obikeze, Z. A. Belay and O. J. Caleb, *Food Biosci.*, 2021, **41**, 100840.
6 T. Farooq, M. Adeel, Z. He, M. Umar, N. Shakoor, W. Da Silva, W. Elmer, J. C. White and Y. Rui, *ACS Nano*, 2021, **15**, 6030–6037.
7 L. Fu, Z. Wang, O. P. Dhankher and B. Xing, *J. Exp. Bot.*, 2020, **71**, 507–519.
8 M. F. Ahmad, F. A. Ahmad, A. A. Alsayegh, M. Zeyaullah, A. M. AlShahrani, K. Muzammil, A. A. Saati, S. Wahab, E. Y. Elbendary, N. Kambal, M. H. Abdelrahman and S. Hussain, *Heliyon*, 2024, **10**, e29128.
9 Z. Yu, T. Lu and H. Qian, *Sci. Total Environ.*, 2023, **888**, 164149.
10 S. Peng and X. Qin, *Ind. Crops Prod.*, 2024, **218**, 119001.
11 R. Saberi Riseh, M. Vatankhah, M. Hassanisaadi and J. F. Kennedy, *Carbohydr. Polym.*, 2023, **309**, 120666.
12 S. Saqib, W. Zaman, F. Ullah, I. Majeed, A. Ayaz and M. F. Hussain Munis, *Appl. Organomet. Chem.*, 2019, **33**, 1–13.
13 Sunera, Z. Khan, M. Irshad, M. Zakria, S. Saqib and W. Zaman, *Microb. Pathog.*, 2024, **197**, 107084.
14 R. Choudhary, A. Kumari, S. Kachhwaha, S. L. Kothari and R. Jain, *S. Afr. J. Bot.*, 2024, **170**, 271–287.
15 S. Lin, C. Xu, S. Hu, X. Chen and F. Wu, *Genome sequencing and analysis reveal the biosynthetic mechanism of anticancer drug terpenoid in Aspergillus tubingensis*, Research Square, 2022, DOI: **10.21203/rs.3.rs-1599234/v1**.
16 S. Nisa, N. Khan, W. Shah, M. Sabir, W. Khan, Y. Bibi, M. Jahangir, U. H. Irshad and S. Alam, *Biol. Sci.*, 2020, **45**, 4477–4487.
17 H. Mohamed, W. Ebrahim, M. El-Neketi, M. F. Awad, H. Zhang, Y. Zhang and Y. Song, *Molecules*, 2002, **27**, 3762.
18 K. Wittstein, A. Cordsmeier, C. Lambert, L. Wendt, E. B. Sir, J. Weber, N. Wurzler, L. E. Petrini and M. Stadler, *Stud. Mycol.*, 2020, **96**, 1–16.

19 N. Selwal, F. Rahayu, A. Herwati, E. Latifah, Supriyono, C. Suhara, I. B. Kade Suastika, W. M. Mahayu, A. K. Wani and J. Agric, *Food Res.*, 2023, **14**, 100702.
20 S. Jadoun, R. Arif, N. K. Jangid and R. K. Meena, *Environ. Chem. Lett.*, 2021, **19**, 355–374.
21 V. Soni, P. Raizada, P. Singh, H. N. Cuong, R. S, A. Saini, R. V. Saini, Q. Van Le, A. K. Nadda, T. T. Le and V. H. Nguyen, *Environ. Res.*, 2021, **202**, 111622.
22 O. Ejeromedoghene, A. Oladipo, O. Oderinde, E. S. Okeke, S. A. Amolegbe, T. M. Obuotor, C. A. Akinremi, S. Adewuyi and G. Fu, *ACS Agric. Sci. Technol.*, 2021, **1**, 664–673.
23 P. Ton-That, T. A. Dinh, H. Thanh Gia-Thien, N. Van Minh, T. Nguyen and K. P. H. Huynh, *Food Hydrocolloids*, 2025, **158**, 110496.
24 Y. A. Alli, M. T. Ogunleye, O. Ejeromedoghene, S. Adewuyi, J. G. Bodunde, F. Balla, O. K. Akiode, P. O. Oladoye, K. S. Oluwole and S. Thomas, *Food Hydrocolloids Health*, 2023, **3**, 100124.
25 Y. Li, L. Zheng, G. Mustafa, Z. Shao, H. Liu, Y. Li, Y. Wang, L. Liu, C. Xu, T. Wang, J. Zheng, F. Meng and Q. Wang, *Food Chem.*, 2024, **454**, 139685.
26 S. Saqib, W. Zaman, A. Ayaz, S. Habib, S. Bahadur, S. Hussain, S. Muhammad and F. Ullah, *Biocatal. Agric. Biotechnol.*, 2020, **28**, 101729.
27 Z. Juan, *Int. J. Nutr. Food Sci.*, 2014, **3**, 111.
28 X. Liu, W. Liao and W. Xia, *Food Hydrocolloids*, 2023, **140**, 108612.
29 C. Duan, X. Meng, J. Meng, M. I. H. Khan, L. Dai, A. Khan, X. An, J. Zhang, T. Huq and Y. Ni, *J. Bioresour. Bioprod.*, 2019, **4**, 11–21.
30 M. H. Sarfraz, S. Hayat, M. H. Siddique, B. Aslam, A. Ashraf, M. Saqalein, M. Khurshid, M. F. Sarfraz, M. Afzal and S. Muzammil, *Prog. Org. Coat.*, 2024, **188**, 108235.
31 E. Charria-Girón, M. C. Espinosa, A. Zapata-Montoya, M. J. Méndez, J. P. Caicedo, A. F. Dávalos, B. E. Ferro, A. M. Vasco-Palacios and N. H. Caicedo, *Front. Microbiol.*, 2021, **12**, 1–14.
32 V. A. Petrova, N. V. Dubashynskaya, I. V. Gofman, A. S. Golovkin, A. I. Mishanin, A. D. Aquino, D. V. Mukhametdinova, A. L. Nikolaeva, E. M. Ivan'kova, A. E. Baranchikov, A. V. Yakimansky, V. K. Ivanov and Y. A. Skorik, *Int. J. Biol. Macromol.*, 2023, **229**, 329–343.
33 S. R. Sinha, A. Singha, M. Faruquee, M. A. S. Jiku, M. A. Rahaman, M. A. Alam and M. A. Kader, *Bull. Natl. Res. Cent*, 2019, **43**, 185.
34 T. V. M. Sreekanth, P. C. Nagajyothi, G. R. Reddy, J. Shim and K. Yoo, *Sci. Rep.*, 2019, **9**, 2–10.
35 A. Miri, M. Darroudi and M. Sarani, *Appl. Organomet. Chem.*, 2020, **34**, 1–7.
36 M. C. Portillo, O. P. Moreno, M. A. Mora-Ramírez, H. J. Santiesteban, C. B. Avendaño and Y. P. Bernal, *Optik*, 2021, **248**, 1–10.
37 A. Butt, J. S. Ali, A. Sajjad, S. Naz and M. Zia, *Biochem. Syst. Ecol.*, 2022, **104**, 104462.
38 N. E. A. El-Naggar, A. M. Shiha, H. Mahrous and A. B. A. Mohammed, *Sci. Rep.*, 2022, **12**, 1–19.
39 E. Paparazzo, *Mater. Res. Bull.*, 2011, **46**, 323–326.
40 M. Ayiania, M. Smith, A. J. R. Hensley, L. Scudiero, J. S. McEwen and M. Garcia-Perez, *Carbon*, 2020, **162**, 528–544.
41 M. Accolla, G. Pellegrino, G. A. Baratta, G. G. Condorelli, G. Fedoseev, C. Scirè, M. E. Palumbo and G. Strazzulla, *Astron. Astrophys.*, 2018, **620**, 1–9.
42 Q. Maqbool, *RSC Adv.*, 2017, **7**, 56575–56585.
43 O. Ejeromedoghene, O. Oderinde, X. Ma, M. Olusola, S. Adewuyi and G. Fu, *J. Mater. Sci.:Mater. Electron.*, 2021, **32**, 16324–16334.
44 G. Eka Putri, Y. Rilda, S. Syukri, A. Labanni and S. Arief, *J. Mater. Res. Technol.*, 2021, **15**, 2355–2364.
45 N. Monica Ahmad and N. Aishah Hasan, *J. Nanotechnol.*, 2023, 1–9.
46 S. M. Al-shimmary, Z. H. Shehab and E. H. Jassim, *Egyptian Journal of Basic and Applied Sciences*, 2025, **12**, 1–16.
47 K. Scherer, W. Soerjawinata, S. Schaefer, I. Kockler, R. Ulber, M. Lakatos, U. Bröckel, P. Kampeis and M. Wahl, *Bioprocess Biosyst. Eng.*, 2022, **45**, 931–941.
48 A. Tabriz, M. A. Ur Rehman Alvi, M. B. Khan Niazi, M. Batool, M. F. Bhatti, A. L. Khan, A. U. Khan, T. Jamil and N. M. Ahmad, *Carbohydr. Polym.*, 2019, **207**, 17–25.
49 J. An, Y. Song, J. Zhao and B. Xu, *Front. Cell. Infect. Microbiol.*, 2023, **13**, 1–13.
50 A. R. Sousa, J. C. Oliveira and M. J. Sousa-Gallagher, *J. Food Eng.*, 2017, **206**, 13–22.
51 Y. Zhao, L. Li, S. Gao, S. Wang, X. Li and X. Xiong, *Lwt*, 2023, **176**, 114497.
52 S. Khalid, S. A. Hassan, H. Javaid, M. Zahid, M. Naeem, Z. F. Bhat, G. Abdi, R. M. Aadil and J. Agric, *Food Res.*, 2024, **15**, 100962.
53 L. Buendía-Moreno, M. Ros-Chumillas, L. Navarro-Segura, M. J. Sánchez-Martínez, S. Soto-Jover, V. Antolinos, G. B. Martínez-Hernández and A. López-Gómez, *Food Bioprocess Technol.*, 2019, **12**, 1548–1558.
54 Y. Gao, L. Jiao, F. Jiao and D. Dong, *LWT–Food Sci. Technol.*, 2022, **155**, 112930.
55 I. M. Taha, A. Zaghlool, A. Nasr, A. Nagib, I. H. El Azab, G. A. M. Mersal, M. M. Ibrahim and A. Fahmy, *Polymers*, 2022, **14**, 1439.